Iranian Journal of Materials Science and Engineering, Vol. 18, Number 3, September 2021
RESEARCH PAPER

Manufacturing and Structural Evaluation of Polymer Derived SiOC/TiC and SiOC/TiC/Mullite Nanocomposites

Amirhosein Paryab[1], Toktam Godary[1], Sorosh Abdollahi[2], Mohsen Anousheh[3], Adrine Malek Khachatourian[1,*]

* *khachatourian@sharif.edu*
[1] Department of Materials Science and Engineering, Sharif University of Technology, Tehran, Iran
[2] School of Metallurgy and Materials Engineering, Iran University of Science and Technology, Tehran, Iran
[3] Department of Materials Science and Engineering, Islamic Azad University Science and Research branch, Tehran, Iran

Received: January 2021 **Revised: June 2021** **Accepted: July 2021**
DOI: 10.22068/ijmse.2093

Abstract: *Silicon oxycarbide (SiOC) materials derived from silicone attracted great attention for their superior high-temperature behavior. In the present study, Si (Ti)OC and Si (Ti,Al)OC nanocomposites, in which alkoxide precursors were used with the main silicone precursor, have been compared with SiOC material. Although in SiOC, C was bonded with Si in a carbon-rich SiOC phase, X-ray diffraction (XRD) and Fourier transform infrared spectroscopy (FTIR) showed that TiC was the preferred state for C atoms upon adding Ti into the system. This claim was also substantiated by Raman spectroscopy, where adding Ti into the system lowered the intensity of the D band, indicating the high affinity of C to form crystalline TiC. In the Si(Ti,Al)OC nanocomposites synthesized by adding AlCl3 into the Si(Ti)OC system, mullite nanocrystals formed a superlattice structure with TiC. UV-vis spectra of the nanocomposites showed Si (Ti,Al)OC with mullite-TiC superlattice had a larger bandgap compared with Si(Ti)OC with only TiC nanocrystals.*

Keywords: *SiOC nanocomposite, mullite, TiC, polymer-derived ceramics.*

1. INTRODUCTION

Polymer-derived ceramics (PDC) have been studied extensively for their potentials for different applications, e.g. electrical, environmental, medical, etc [1-3]. Among the PDC materials, silicon-based PDC, especially silicon oxycarbide (SiOC) materials synthesized via polymer to the ceramic conversion of polysiloxanes, have also gained enormous interest due to their advanced structural and functional applications. The structure of SiOC glass and glass-ceramics contain a mixed bonded of SiO_xC_{4-X} tetrahedral units sharing their corners. O corners can only be shared between two tetrahedral units, while C corners can develop corner-sharing with four tetrahedral units. Therefore, glassy SiOC consists of a more cross-linked network in comparison to a fully connected SiO_2 network. Moreover, this type of C atoms contribution within the structure of SiOC enhances glass transition temperature, hardness, and Young's modulus effectively, compared to silica glass [4-8].
For polymer-derived SiOC, heat treatment has an essential role in the phase evolution of SiOC. At temperatures up to 1000°C, the amorphous SiOC is evident, whereas phase separation to O-rich SiOC, C-rich SiOC, SiO_2, and "free carbon" starts at higher temperatures. At temperatures above 1300°C, the amorphous silica phase reacts with carbon forming silicon carbide and gaseous CO [9].
The characteristics of silicon-based materials were tuned by additional elements such as B [10], Al [11, 12], Ti [12, 13], Zr [15-17], Hf [18], Ce [19], Sn [20], and Sb [21], and novel hybrid siloxane-oxide materials were manufactured via sol-gel derived or polymer-derived methods. In sol-gel derived synthesis, different elements could be introduced to the SiOC matrix by metal-alkoxides incorporated with polysiloxane to form hybrid xerogels [22-24]. However, the NMR study of the mentioned hybrid materials pointed out due to the nature of used metal-alkoxides various Si-O-Me (Me= metallic atom) bonds could be formed [24]. Dire et al. [25] investigated the microstructural and structural evolution during the pyrolysis of sol-gel derived hybrid polydimethylsiloxane-titania materials. The liquid state NMR study of the hydrolysis-condensation process of mentioned

[DOI: 10.22068/ijmse.2093]

nanocomposites showed that Si-O-Ti bonds were redistributed, forming Ti-O-Ti and Si-O-Si bonds. Due to the higher affinity of Ti toward carbon compared to Si, the possibility of SiC formation is reduced during heat treatment; meanwhile, the formation of titanium carbide (TiC) was facilitated, which could alter the different properties of the synthesized nanocomposite.
In this investigation, SiOC/TiC nanocomposites were synthesized via the PDC method, and the structural, microstructural, and optical bandgap characteristics were studied. Furthermore, the effect of Al addition on the phase evolution of fabricated nanocomposites was also assessed.

2. EXPERIMENTAL PROCEDURE

2.1. Materials

Commercial room temperature vulcanizing (RTV2) silicone resin (PDMS) with a 56.6 wt% ceramic yield, which accompanied a hardener, was used in this work. Other chemical reagents were TTIP (CAS 546-68-9), AlCl3 (CAS 7446-70-0), and ethanol (CAS 64-17-5), which were purchased from Merck and used without further treatment.

2.2. Sample preparation

Three samples (SiOC, Si(Ti)OC, Si(Ti,Al)OC) were prepared according to Table 1. Firstly, the stoichiometry amount of $AlCl_3$ was mixed with 25 wt% ethanol and stirred for ten minutes. Then the prepared solution was added to TTIP and stirred again for three minutes.

Table 1. Samples composition.

Sample name	Silicone (wt%)	TTIP (wt%)	$AlCl_3$ (wt%)
SiOC	100	-	-
Si(Ti)OC	70	30	-
Si(Ti,Al)OC	70	20	10

Subsequently, the mixture was mixed with silicone, and the whole batch was heated to 60 ºC and stirred for ten minutes. After that, an appropriate amount of distilled water (5 wt% of TTIP) was added into the stirring mixture dropwise, and stirring continued for another three minutes. Finally, resin hardener at the amount of 5 wt% of silicone was added inside the beaker, and stirring stopped after three minutes. Each batch was poured inside aluminum foil handmade cups and cured at 60ºC for 24 hours after being vacuumed in 10^{-2} mbar pressure. After that, the samples were removed from the cups and undergone heat treatment by such a program: reaching to 450°C in 4 hours, being hold at 450°C for 4 hours soaking time, reaching to 1300°C in 4 hours, and being hold at 1300°C for 4 hours soaking time. Ar gas (99.99%) with a 1.1 L/hour flow rate was used during the heat treatment process.

2.3. Physical and structural assessment

FT-IR analysis (Vertex 70 FT-IR spectrometer, Bruker), Transition Electron Microscopy (Philips CM-200), High-Resolution Transition Electron Microscopy (FEI-TEC9G20, 200 kV), and UV-vis analysis (Cary 100 UV-visible Spectrophotometer, Agilent Technologies) was carried out for microstructural and structural assessment. Furthermore, X-Ray Diffraction analysis (Panalytical-2009) with a lamp of Cu Kα radiation (λ = 0.15418 nm) was used to evaluate the crystalline and amorphous phases. A Raman spectroscopy (Teksan co) equipped with an Ar laser (λ = 514.5 nm) was used to evaluate carbon states inside the structure.

3. RESULTS AND DISCUSSION

To prepare nanocomposites via the PDC method, the incorporation of precursors in the atomic scale before heat treatment is essential. Thus, the evaluation of FTIR spectra for all samples before and after heat treatment at 1300ºC was conducted (Fig.1). According to Fig.1(a) for SiOC, Si (Ti)OC, and Si(Ti,Al)OC precursors, Si-O-C (1024 cm^{-1}), Si-O-Si (1093 cm^{-1}) [25], and Si-CH_3 adsorption bonds ($\delta(CH_3)$=1263 cm^{-1}, δ(Si-C)=802 cm^{-1}) [26] were evident and were all attributed to silicone resin. In Si (Ti)OC precursor no peaks regarding the Ti-O band (around 750 cm^{-1}) were detected, probably this peak was masked by a wide Si-CH_3 peak at the same region [27]. In the Si (Ti,Al)OC precursor, the peak at 500 and 700 cm^{-1} are attributed to the Al-O bond [28]. Although there was no sign of Ti-C bond (998 cm^{-1}) in precursors spectra, it was obvious after heat treatment, this peak appears, especially for Si (Ti) OC sample (Fig.1(b)). Moreover, the peak intensity at 750 cm^{-1} attributed to the Si-C bond [29] had been weakened for Si(Ti)OC and Si(Ti,Al)OC samples in comparison with SiOC sample, indicating higher affinity of Ti toward carbon, compared to Si.

[DOI: 10.22068/ijmse.2093]

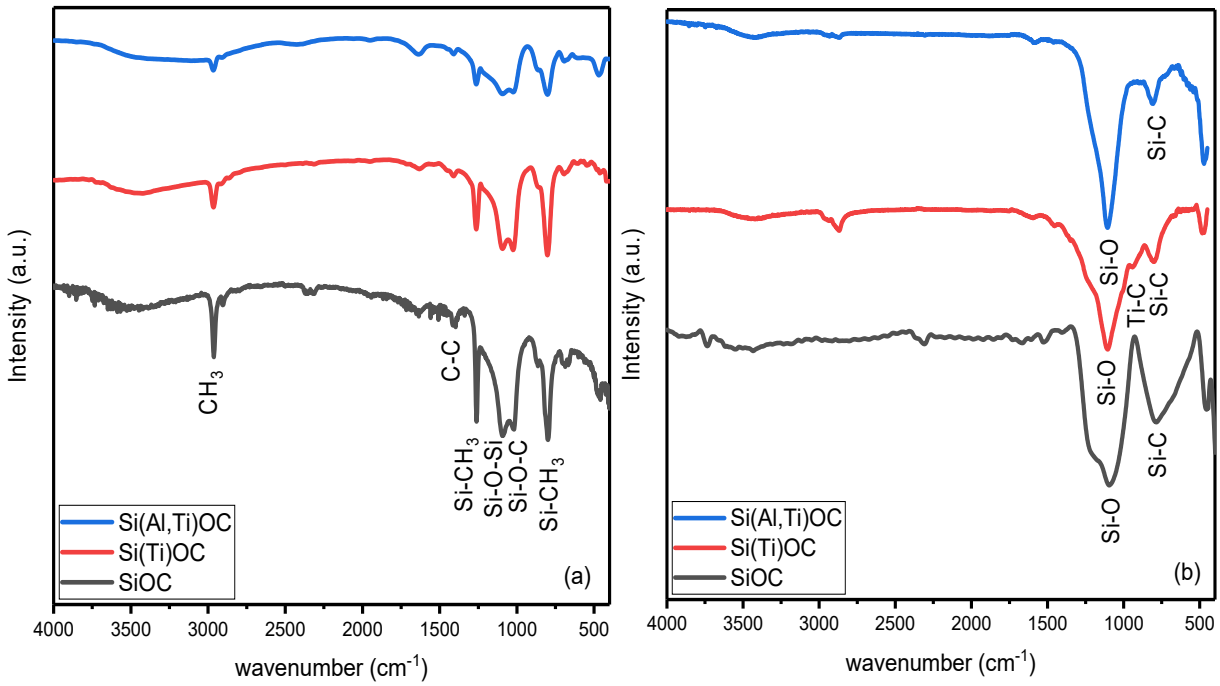

Fig. 1. FTIR spectra of (a) SiOC, Si(Ti)OC, and Si(Ti,Al)OC precursors, and (b) SiOC, Si(Ti)OC, and Si(Ti,Al)OC samples after heat treatment at 1300°C.

Fig.2 shows XRD patterns of SiOC, Si (Ti) OC, and Si(Ti,Al)OC samples after heat treatment at 1300ºC. It was observed that the XRD pattern of SiOC consists of two broad peaks referring to O-rich SiOC and C-rich SiOC phases at 22° and 35°, respectively, without any sharp peaks attributing to crystalline phases. In contrast, the formation of crystalline mullite and TiC phases were evident for Si (Ti)OC and Si(Ti,Al)OC samples. As mentioned previously, in the FTIR spectra of Si (Ti)OC and Si(Ti,Al)OC samples, the Ti-C bond appeared after heat treatment.

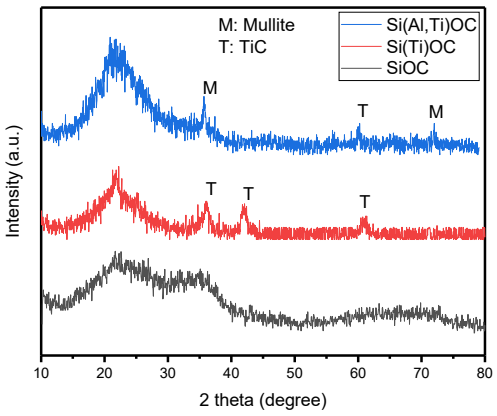

Fig. 2. XRD patterns of SiOC, Si(Ti)OC, and Si(Ti,Al)OC samples after heat treatment at 1300°C.

XRD results also confirmed the TiC phase existence.

It has been reported that in lower temperatures, titanium oxide nanocrystals were formed [25], whereas by increasing heat treatment temperature or soaking time, a progressive transformation of TiO_2 into TiC nanocrystals was facilitated [30].

In Fig.2, it was observed that C-rich SiOC peaks have vanished for Si (Ti)OC and Si(Ti,Al)OC samples. Actually, in high temperatures, due to the greater affinity of Ti toward carbon in comparison to Si, the formation of TiOC structure and eradication of C-rich SiOC were dominant [31].

Fig.3 shows TEM and HRTEM micrographs of SiOC, Si(Ti)OC, and Si(Ti,Al)OC samples. According to Fig.3(a), an amorphous texture is evident for SiOC, whereas dark spots distributed in the texture of Si(Ti)OC are attributed to the crystalline phases (Fig.3(b)). Moreover, Fig.3(c) shows an accumulated form of crystallites in the texture of Si(Ti,Al)OC.

HRTEM micrograph of the SiOC sample illustrates amorphous texture without any orientation (Fig.3(d)), while for Si(Ti)OC sample, a connected network of TiC nanoparticles with d spacing equal to 2.5 A° refers to (111) planes are observed (Fig.3(e)). Si(Ti,Al)OC sample had a

[DOI: 10.22068/ijmse.2093]

superlattice of mullite and TiC (Fig.3(f)) where TiC nanoparticles were separated by mullite nanoparticles with d spacing equal to 3.39 A° referring to (001) planes. HRTEM images also confirmed the structural characterization by XRD results.

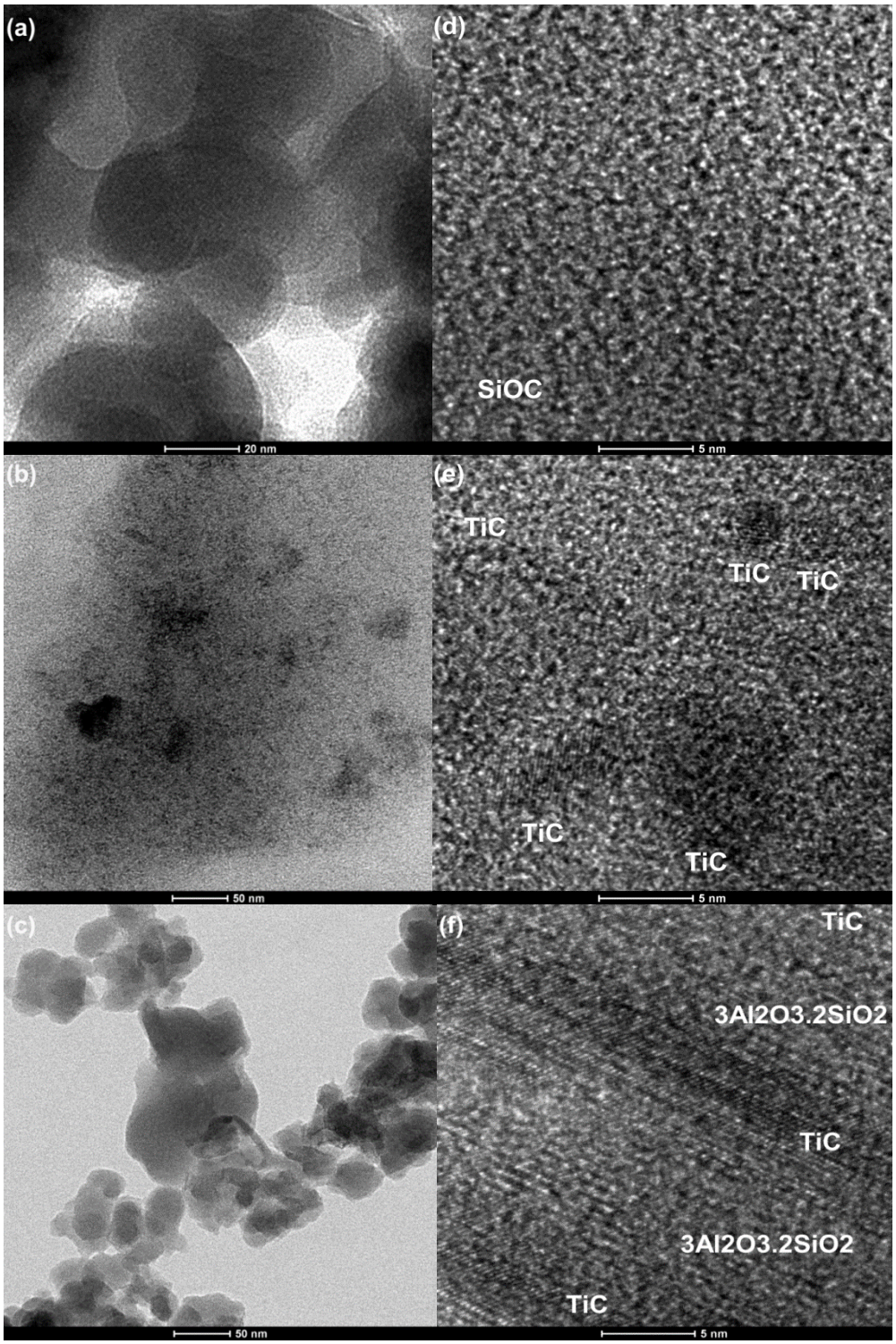

Fig. 3. TEM micrographs of (a) SiOC, (b) Si(Ti)OC and (c) Si(Ti,Al)OC samples, and HRTEM micrographs of (d) SiOC, (e) Si(Ti)OC and (f) Si(Ti,Al)OC samples.

[DOI: 10.22068/ijmse.2093]

Fig.4(a) shows UV-vis adsorption spectra of SiOC, Si(Ti)OC and Si(Ti,Al)OC samples. The spectrum of SiOC shows a sharp adsorption band from 225 to 250 nm. In fact, in amorphous semiconductors, sharp edges are due to the localization of energy states and structural defects [32]. In contrast, Si (Ti)OC and Si(Ti,Al)OC samples show broad adsorption edges at 220-260 nm. For Si(Ti)OC sample, the peak at 220-260 nm would be attributed to TiC [33]; Thus, according to the Tauc plot analysis, the bandgap for such structure is 4.40 eV (Fig4(b)). However, for Si (Ti,Al)OC sample, the peak at 220-260 nm consists of two shoulders referring to TiC and mullite phases [34]. Thus, according to the Tauc plot, the bandgap for such a structure is 4.92 eV (Fig4(b)), which is greater than the bandgap of the Si(Ti)OC sample.

HRTEM micrographs could verify UV-vis results. The HRTEM image of Si (Ti,Al)OC samples displayed the contact breakdown between TiC particles by mullite nanoparticles, producing a superlattice of mullite/TiC.

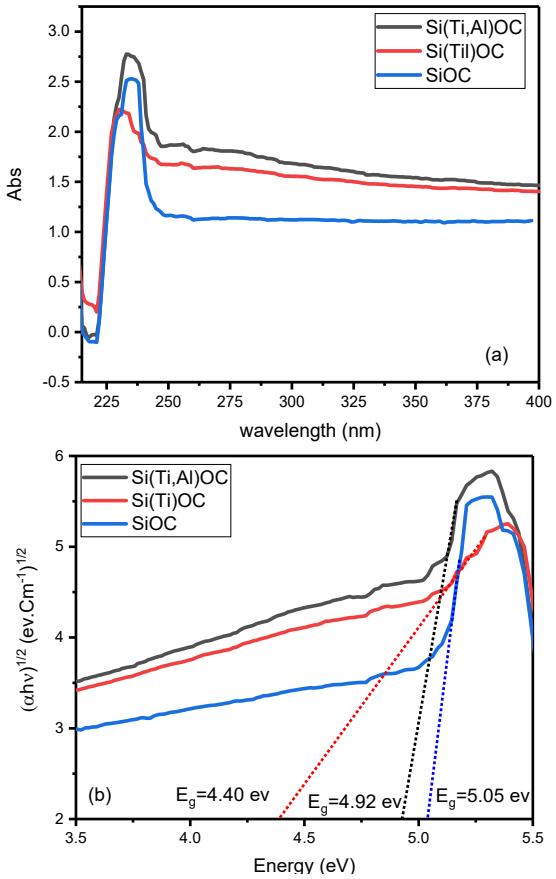

Fig. 4. (a) UV-vis absorption spectra and (b) Tauc plot of Si(Ti)OC, Si(Ti,Al)OC and SiOC samples.

Thus such a microstructure could result in a higher bandgap in comparison to Si (Ti)OC with connected TiC nanocrystals network. TiC is a non-stoichiometric compound, and its properties such as electrical conductivity, chemical stability, and mechanical strength can be tuned by its stoichiometry. Unlike mullite, TiC is an electrically conductive material [35]; therefore, a smaller bandgap of Si(Ti)OC in comparison to Si(Ti,Al)OC is expected.

The seg¬¬regation of carbon was evaluated by Raman spectroscopy. As shown in Fig.5, the D and G characteristics peaks located at about 1351 cm^{-1} and 1598 cm^{-1} are referring to carbon phases [36, 37].

The D band induced by in-plane breathing vibration of the ring structure with A_{1g} symmetry corresponds to any disordered carbon, mainly amorphous nanoclusters of carbon. Thus this band is not available for crystalline forms like graphite [38].

The G band induced by in-plain stretching vibration of SP_2 carbon with E_{2g} symmetry could be affected by carbon allotrope arrangements like graphite [39, 40].

In other words, the D band introduces the segregation of nanoclusters of disordered carbon with SP_3 hybridization, while the G band introduces the segregation of crystalline nanoclusters with SP_2 hybridization. According to Fig.5, the D to G band ratio becomes lower upon adding Ti into the SiOC system, indicating the high affinity of Ti toward carbon to form TiC and decreases the chance to find free carbon in the structure.

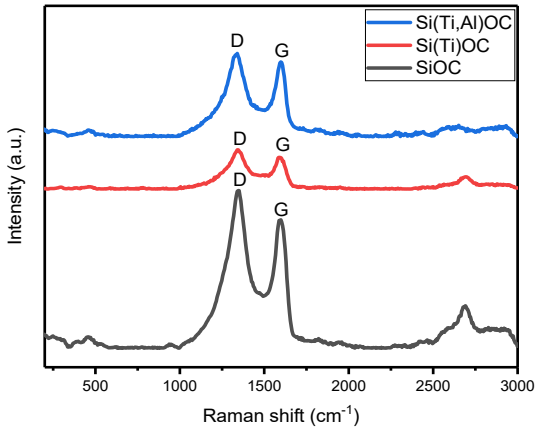

Fig. 5. Raman spectra of SiOC, Si(Ti)OC, and Si(Ti,Al)OC samples.

[DOI: 10.22068/ijmse.2093]

4. CONCLUSIONS

Three SiOC based nanocomposites (SiOC, Si (Ti)OC, and Si(Ti,Al)OC) were prepared via the PDC method. In SiOC nanocomposite, two noncrystalline phases appeared with one rich in disordered Si-C bonds and one rich in Si-O bonds. Upon adding TTIP as an extra precursor in the synthesis stage, Si (Ti)OC nanocomposite was fabricated where disordered C preferred to bond with Ti instead of Si, formed TiC nanocrystals in the matrix of SiOC. For the synthesis of Si (Ti,Al)OC nanocomposite, $AlCl_3$ and TTIP precursors were used. XRD analysis confirmed the presence of mullite crystals along with TiC crystals. HRTEM structural assessments showed a disordered network of atoms in the SiOC phase with no evidence of crystalline structure, whereas in Si(Ti)OC system, nanocrystals of TiC formed a connected network leading to a lower bandgap of this nanocomposite. In Si (Ti,Al)OC nanocomposite mullite crystals formed a superlattice structure with TiC crystals that results in a wider bandgap compared with Si(Ti)OC nanocomposites.

REFERENCES

[1] Riedel, R., Mera, G., Hauser, R., & Klonczynski, A. " Silicon-based polymer-derived ceramics: synthesis properties and applications-a review dedicated to Prof. Dr. Fritz Aldinger on the occasion of his 65th birthday". J. Ceramic Society of Japan. 2006. 114(1330), 425-444.

[2] Paryab, AH., Abdollahi, S., Khalilifard, R., Madaah Hosseini, HR., "Porous Slow Release Silicate-Phosphate Glasses Synthesized By Polymer-Derived Ceramics Method Appropriate For Plants Nourishment". Iranian Journal of Materials Science and Engineering. 2021, 18(1), 80-90.

[3] Abdollahi, S., Paryab, AH., Khalilifard, R., Anousheh, M., Khachatourian, AM., "The fabrication and characterization of bioactive Akermanite/Octacalcium phosphate glass-ceramic scaffolds produced via PDC method". Ceramics International. 2021, 47(5), 6653-6662.

[4] Widgeon, S. J., S. Sen, G. Mera, E. Ionescu, R. Riedel, and A. Navrotsky. "29Si and 13C solid-state NMR spectroscopic study of nanometer-scale structure and mass fractal characteristics of amorphous polymer derived silicon oxycarbide ceramics." Chemistry of Materials 2010, 23, 6221-6228.

[5] Saha, A., Raj, R., Williamson, DL., "A model for the nanodomains in polymer-derived SiCO" J. American Ceramic Society. 2006, 89(7), 2188-2195.

[6] Sen, S., Widgeon, S., "On the mass fractal character of Si-based structural networks in amorphous polymer derived ceramics". Nanomaterials. 2015, 5(1), 366-375.

[7] Rouxel, T., Massouras, G., Sorarù, GD., "High temperature behavior of a gel-derived SiOC glass: Elasticity and viscosity". J. sol-gel science & technology. 1999, 14(1), 87-94.

[8] Yamamoto, K., Ohshita, J., Mizumo, T., Tsuru, T., "Efficient synthesis of SiOC glasses from ethane, ethylene, and acetylene-bridged polysilsesquioxanes". J. Non-Crystalline Solids. 2015, 408, 137-141.

[9] Stabler, C., Ionescu, E., Graczyk Zajac, M., Gonzalo Juan, I., Riedel, R., "Silicon oxycarbide glasses and glass-ceramics:“All-Rounder” materials for advanced structural and functional applications". J. American Ceramic Society. 2018, 101(11), 4817-4856.

[10] Ngoumeni-Yappi, R., Fasel, C., Riedel, R., Ischenko, V., Pippel, E., Woltersdorf, J., Clade, J., "Tuning of the rheological properties and thermal behavior of boron-containing polysiloxanes". Chemistry of Materials. 2008, 20(11), 3601-3608.

[11] Abdollahi, S., Paryab, A., Rahmani, S., Akbari, M., Sarpoolaky, H., "Synthesis of $SiOC/Al_2O_3$ nano/macro composites through PDC method; investigation of potentials as layers of a packed bed reactor membrane". Ceramics International. 2020, 46(11), 19000-19007.

[12] Riedel, R., Toma, L., Fasel, C., Miehe, G., "Polymer-derived mullite–SiC-based nanocomposites". J. European Ceramic Society. 2009, 29(14), 3079-3090.

[13] Gregori, G., Kleebe, HJ., Readey, DW., Sorarù, GD., "Energy Filtered TEM Study of Ostwald Ripening of Si Nanocrystals in

[DOI: 10.22068/ijmse.2093]

a SiOC Glass". J. American Ceramic Society. 2006, 89(5), 1699-1703.

[14] Hönack, F., Riedel, R., "Influence of Ti-Based Fillers on the Thermal Decomposition and Phase Development of Polysiloxane Derived Materials". Advanced Engineering Materials. 2003, 5(3), 122-125.

[15] Bhaskar, S., Awin, EW., Kumar, KH., Lale, A., Bernard, S., Kumar, R., "Design of nanoscaled heterojunctions in precursor-derived t-ZrO_2/SiOC(N) nanocomposites: Transgressing the boundaries of catalytic activity from UV to visible light". Scientific reports. 2020, 10(1), 1-3.

[16] Dirè, S., Ceccato, R., Gialanella, S., Babonneau, F., "Thermal evolution and crystallization of polydimethylsiloxane–zirconia nanocomposites prepared by the sol–gel method". J. European Ceramic Society. 1999, 19(16), 2849-2858.

[17] Ionescu, E., Linck, C., Fasel, C., Müller, M., Kleebe, HJ., Riedel, R., "Polymer-derived SiOC/ZrO_2 ceramic nanocomposites with excellent high temperature stability". J. American Ceramic Society. 2010, 93(1), 241-250.

[18] Ionescu, E., Papendorf, B., Kleebe, HJ., Poli, F., Müller, K., Riedel, R., "Polymer-derived silicon oxycarbide/hafnia ceramic nanocomposites. Part I: phase and microstructure evolution during the ceramization process". J. American Ceramic Society. 2010, 93(6), 1774-1782.

[19] García, B., Casado, E., Tamayo, A., "Synthesis and characterization of Ce/SiOC nanocomposites through the polymer derived ceramic method and evaluation of their catalytic activity". Ceramics International. 2020, 46(2), 1362-1373.

[20] Dubey, RJ., Sasikumar, PV., Krumeich, F., Blugan, G., Kuebler, J., Kravchyk, KV., Graule, T., Kovalenko, MV., "Silicon Oxycarbide—Tin Nanocomposite as a High Power Density Anode for Li-Ion Batteries". Advanced Science. 2019, 6(19), 1901220.

[21] Dubey, RJ., Sasikumar, PV., Cerboni, N., Aebli, M., Krumeich, F., Blugan, G., Kravchyk, KV., Graule, T., Kovalenko MV., "Silicon oxycarbide-antimony nanocomposites for high-performance Li-ion battery anodes". Nanoscale. 2020, 12(25), 13540-13547.

[22] Sun, J., Wen, QB., Li, T., Wiehl, L., Fasel, C., Feng, Y., De Carolis, D., Yu, ZJ., Fu, QG., Riedel, R., "Phase evolution of SiOC-based ceramic nanocomposites derived from a polymethylsiloxane modified by Hf and Ti alkoxides". J. American Ceramic Society. 2020, 103(2), 1436-1445.

[23] Martos, C., Rubio, F., Rubio, J., Oteo, JL., "Infiltration of SiO2/SiOC Nanocomposites by a Multiple Sol Infiltration-Pyrolysis Process". Journal of sol-gel science and technology. 2003, 26(1), 511-516.

[24] Guermeur, C., Lambard, J., Gerard, JF., Sanchez, C., "Hybrid polydimethylsiloxane-zirconium oxo nanocomposites. Part 1 Characterization of the matrix and the siloxane-zirconium oxo interface". J. Materials Chemistry. 1999, 9(3), 769-778.

[25] Dirè, S., Ceccato, R., Babonneau, F., "Structural and microstructural evolution during pyrolysis of hybrid polydimethylsiloxane-titania anocomposites". J. sol-gel science & technology. 2005, 34(1), 53-62.

[26] Bellamy, LJ., The infra-red spectra of complex molecules, Chapter 20, Organo-Silicon compounds. Chapman & Hall. ed. 3rd, 1975, UK London, 374-383.

[27] Liu, Z., Jian, Z., Fang, J., Xu, X., Zhu, X., Wu, S., "Low-temperature reverse microemulsion synthesis, characterization, and photocatalytic performance of nanocrystalline titanium dioxide". Int. J. Photoenergy. 2012, 2, 12-20.

[28] Liu, C., Shih, K., Gao, Y., Li, F., Wei, L., "Dechlorinating transformation of propachlor through nucleophilic substitution by dithionite on the surface of alumina". J. soils and sediments. 2012, 12(5), 724-733.

[29] Nakamoto, K., Handbook of Vibrational Spectroscopy, chapter 2, Infrared and Raman Spectra of Inorganic and Coordination Compounds, ed 1st, John Wiley & Sons, UK London, 2006, 193-274.

[30] Dire, S., Babonneau, F., "Structural evolution during pyrolysis of sol-gel

[DOI: 10.22068/ijmse.2093]

derived hybrid materials". J. Sol-Gel Science & Technology. 1994, 2(1), 139-142.
[31] Babonneau, F., Barre, P., Livage, J., Verdaguer, M., "Spectroscopic Characterization of a Pre-Ceramic Polymer For Sic/Tic System". MRS Online Proceedings Library Archive. 1990, 27,180.
[32] Adachi, S., Optical properties of crystalline and amorphous semiconductors: Materials and fundamental principles, Chapter 4, The interband transition region: Amorphous & microcrystalline materials. Springer Science & Business Media, ed. 1st, 1999, U.S. New York, 131-175.
[33] Corradetti, S., Carturan, SM., Maggioni, G., Franchin, G., Colombo, P., Andrighetto, A., "Nanocrystalline titanium carbide/carbon composites as irradiation targets for isotopes production". Ceramics International. 2020, 46(7), 9596-9605.
[34] Li, C., Sun, Z., Liu, L., Huang, W., Zheng, S., "Facile synthesis and enhanced visible-light photoactivity of a gC3N4/mullite composite". RSC advances. 2016, 6(93), 91002-91011.
[35] Galevsky, GV., Rudneva, VV., Garbuzova, AK., Valuev, DV., "Titanium carbide: nanotechnology, properties, application". IOP conference series: materials science and engineering 2015, 91(1), 12-17).
[36] Domnich, V., Reynaud, S., Haber, RA., Chhowalla, M., "Boron carbide: structure, properties, and stability under stress". J. American Ceramic Society. 2011, 94(11), 3605-3628.
[37] Wang, C., Huang, F., Jiang, Y., Zhou, Y., Du, L., "A Novel Oxidation Resistant SiC/B4C/C Nanocomposite Derived from a Carborane-Containing Conjugated Polycarbosilane". J. American Ceramic Society. 2012, 95(1), 71-74.
[38] Rosenburg, F., Ionescu, E., Nicoloso, N., Riedel, R., "High-temperature Raman spectroscopy of nano-crystalline carbon in silicon oxycarbide". Materials. 2018, 11(1), 93.
[39] Thomsen, C., Reich, S., "Double resonant Raman scattering in graphite". Physical review letters. 2000, 85(24), 5214.
[40] Nemanich, RJ., Solin, SA., "First-and second-order Raman scattering from finite-size crystals of graphite". Physical Review B. 1979, 20(2), 392.

[DOI: 10.22068/ijmse.2093]